First Interchain Peptide Interaction Detected by ESR in Fully Synthetic, Template-Assisted, Two-Helix Bundles

Alessandra Polese,[†] D. Joe Anderson,[‡] Glenn Millhauser,*[,‡] Fernando Formaggio,[†] Marco Crisma,[†] Fernando Marchiori,[†] and Claudio Toniolo*[,†]

Contribution from the Department of Chemistry and Biochemistry, University of California at Santa Cruz, Santa Cruz, California 95064, and Biopolymer Research Center, CNR, Department of Organic Chemistry, University of Padova, 35131 Padova, Italy

Received June 18, 1999. Revised Manuscript Received September 17, 1999

Abstract: We have designed and synthesized by solution methods two simple two-helix bundles based on a conformationally constrained cyclo-dipeptide template to the side chains of which two short, 2,2,6,6-tetramethylpiperidine-1-oxyl-4-amino-4-carboxylic acid spin-monolabeled, 3_{10}-helical peptides are covalently tethered. The preferred conformation of the appended chains has been assessed by FTIR absorption. The conclusions are corroborated by an X-ray diffraction analysis of one of the terminally blocked pentapeptide tails. For the first time, a solvent-dependent, inter-helix interaction has been monitored by conventional ESR spectroscopy on *fully synthetic* peptide systems. Half-field ESR measurements of these side-chain-substituted templates provided an experimental average distance between the two labels that is in good accord with that determined in a molecular modeling study.

Introduction

Nitroxide-based, spin *mono*-labeled peptide and protein variants are currently extensively investigated by electron spin resonance (ESR) and fluorescence quenching techniques to assess a variety of properties, including 3D structure; conformational transition; self-association tendency; local and global mobilities; conservation of subunit interface and overall topology in multiple-helix bundles; accessibility of functional groups; interaction with small ligands, metal ions, surfactants, and receptors; immersion depth and orientation into biological and model membranes; and gating mechanism.[1]

On the other hand, ESR studies of spin−spin interactions of *double* nitroxide-labeled peptides and proteins have recently provided relevant information on the precise conformation and stability of turns and helices and on intrahelix residue−residue distances (ESR *spectroscopic ruler*).[2]

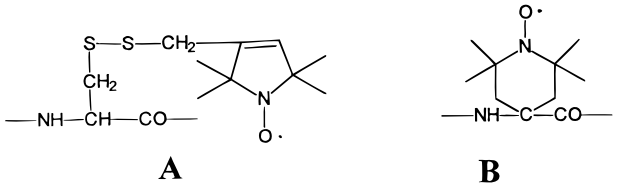

A **B**

Figure 1. Structures of a typical side-chain spin label Cys (**A**) and TOAC (**B**).

Commonly, the nitroxide label is introduced into a *flexible* Cys side chain through a *flexible* spacer arm (Figure 1A) after total chemical synthesis or site-directed mutagenesis of the peptide or protein target. More recently, we have shown that significantly stronger spin−spin interactions may be provided by polypeptide systems based on two residues of the side-chain *conformationally restricted, strongly helicogenic*, C^{α}-tetrasubstituted α-amino acid 2,2,6,6-tetramethylpiperidine-1-oxyl-4-

[†] University of Padova.

[‡] University of California at Santa Cruz.

(1) Millhauser, G. L. *Trends Biochem. Sci.* **1992**, *17*, 448−452. (b) Pertinhez, T. A.; Nakaie, C. R.; Paiva A. C. M.; Schreier, S. *Biopolymers* **1997**, *42*, 821−829. (c) Altenbach, C.; Greenhalgh, D. A.; Khorana, H. G.; Hubbell, W. L. *Proc. Natl. Acad. Sci. U.S.A.* **1994**, *91*, 1667−1671. (d) Hubbell, W. L.; Altenbach, C. *Curr. Opin. Struct. Biol.* **1994**, *4*, 566−573. (e) Ottemann, K. M.; Thorgeirsson, T. E.; Kolodziej, A. F.; Shin, Y.-K.; Koshland, D. E., Jr. *Biochemistry* **1998**, *37*, 7062−7069. (f) Jackson, A. E.; Harris, T. M.; Puett, D. *J. Protein Chem.* **1987**, *6*, 497−515. (g) Brandenburg, D.; Fabry, M.; Engels, N.; Kleinjung, J.; Strack, U.; Thevis, W. In *Peptides 1996*; Ramage, R., Epton, R., Eds.; Mayflower Sci.: Kingswinford, England, 1998; pp 101−104. (h) Stopar, D.; Jansen, K. A. J.; Pali, T.; Marsh, D.; Hemminga, M. *Biochemistry* **1997**, *36*, 8261−8268. (i) Victor, K.; Cafiso, D. S. *Biochemistry* **1998**, *37*, 3402−3410. (j) Johansson, J. S.; Gibney, B. R.; Rabanal, F.; Reddy, K. S.; Dutton, P. L. *Biochemistry* **1998**, *37*, 1421−1429. (k) Koteiche, H. A.; Berengian, A. R.; Mehaourab, H. S. *Biochemistry* **1998**, *37*, 12681−12688. (l) Klug, C. S.; Eaton, S. S.; Eaton, G. R.; Feix, J. B. *Biochemistry* **1998**, *37*, 9016−9023. (m) Török, M.; Hideg, K.; Dux, L.; Horvath, L. *J. Mol. Struct.* **1997**, *408/409*, 177−180. (n) Subczynski, W. K.; Lewis, R. N. A. H.; McElhaney, R. N.; Hodges, R. S.; Hyde, J. S.; Kusumi, A. *Biochemistry* **1998**, *37*, 3156−3172. (o) Griffith, O. H.; Waggoner, A. S. *Acc. Chem. Res.* **1969**, *2*, 17−24. (p) Pispisa, B.; Palleschi, A.; Stella, L.; Venanzi, M.; Toniolo, C. *J. Phys. Chem.* **1998**, *B102*, 7890−7898. (q) Monaco, V.; Formaggio, F.; Crisma, M.; Toniolo, C.; Hanson, P.; Millhauser, G. *Biopolymers* **1999**, *50*, 239−253.

(2) (a) Miick, S. M.; Martinez, G. V.; Fiori, W. R.; Todd, A. P.; Millhauser, G. L. *Nature* **1992**, *359*, 653−655. (b) Millhauser, G. L. *Biochemistry* **1995**, *34*, 3873−3877. (c) Smithe, M. L.; Nakaie, C. R.; Marshall, G. R. *J. Am. Chem. Soc.* **1995**, *117*, 10555−10562. (d) He, M. M.; Voss, J.; Hubbell, W. L.; Kaback, H. R. *Biochemistry* **1997**, *36*, 13682−13687. (e) Rabenstein, M. D.; Shin, Y. K. *Proc. Natl. Acad. Sci. U.S.A.* **1995**, *92*, 8239−8243. (f) Saxena, S.; Freed, J. H. *Chem. Phys. Lett.* **1996**, *251*, 102−110. (g) Sankarapandi, S.; Sukumar, M.; Balaram, P.; Manoharan, P. T. *Biochem. Biophys. Res. Commun.* **1995**, *213*, 439−446. (h) Wertz, S. L.; Savino, Y.; Cafiso, D. S. *Biochemistry* **1996**, *35*, 11104−11112. (i) Monaco, V.; Formaggio, F.; Crisma, M.; Toniolo, C.; Hanson, P.; Millhauser, G. L.; George, C.; Deschamps, J. R.; Flippen-Anderson J. L. *Bioorg. Med. Chem.* **1999**, *7*, 119−131. (j) Hanson, P.; Martinez, G.; Millhauser, G. L.; Formaggio, F.; Crisma, M.; Toniolo, C.; Vita, C. *J. Am. Chem. Soc.* **1996**, *118*, 271−272. (k) Hanson, P.; Millhauser, G.; Formaggio, F.; Crisma, M.; Toniolo, C. *J. Am. Chem. Soc.* **1996**, *118*, 7618−7625. (l) Toniolo, C.; Valente, E.; Formaggio, F.; Crisma, M.; Pilloni, G.; Corvaja, C.; Toffoletti, A.; Martinez, G. V.; Hanson, M. P.; Millhauser, G.; George, C.; Flippen-Anderson, J. L. *J. Pept. Sci.* **1995**, *1*, 45−57. (m) Hanson, P.; Anderson, D. J.; Martinez, G.; Millhauser, G. L.; Formaggio, F.; Toniolo, C.; Vita, C. *Mol. Phys.* **1998**, *95*, 957−966.

10.1021/ja992079h CCC: $18.00
Published on Web 11/18/1999

amino-4-carboxylic acid (TOAC), which is characterized by a stable nitroxide moiety partially incorporated into the six-membered ring side chain (Figure 1B).[2i−m,3]

In the present study, we monitored for the first time by ESR the onset of an intramolecular inter-helix spin−spin interaction in *fully synthetic*, simple models based on multiple (two)-helix peptide bundles. The models are characterized by a semi-rigid template, the 2,5-diketopiperazine (DKP) cyclo-(Glu-Glu),[4] and by two identical, aligned in parallel, putative helical peptide tails. The DKP bis(carboxylic acid) platform, because of the cis geometry imparted by the two homo-chiral components of the six-membered ring, provides a unique opportunity to systematically alter the side-chain substituents while holding the orientation between them fixed relative to acyclic analogues. The N-terminal amino function of each tail is covalently linked to a Glu γ-carboxylic function of the DKP scaffold via an amide bond. In the two pentapeptide chains of **2**, a single, guest TOAC residue was incorporated in the central position of an α-aminoisobutyric acid (Aib) host homo-peptide chain. The presence of five C^{α}-*tetra*substituted α-amino acids in this pentapeptide allowed us to be confident that a rather stable 3_{10}-helical conformation[5] forms under appropriate experimental conditions.[6] In the side-chain bis-substituted template, **3**, two Aib residues (in positions 2 and 4) were replaced by the weaker helix-inducing, C^{α}-*tri*substituted α-amino acid Ala.[6] For a comparative analysis, the linear pentapeptide model Ac-TOAC-Aib_2-TOAC-Aib-O*t*Bu (**1**) (Ac, acetyl; O*t*Bu, *tert*-butoxy) was also synthesized. Our conformational study of peptides **1**−**3** was forced to rely heavily on infrared (IR) absorption and X-ray diffraction techniques (the latter for the linear model peptide **1**). Indeed, for TOAC-containing short peptides, neither ^{1}H NMR (nuclear magnetic resonance) nor CD (circular dichroism) analysis is informative due to a paramagnetic (nitroxide) line broadening effect in the ^{1}H NMR spectra[7] and a serious overlapping of optically active electronic transitions from the nitroxide and peptide chromophores in the CD curves.[2l] The intramolecular inter-helix spin−spin interaction and distance were determined in peptides **2** and **3** by conventional and half-field measurements, respectively. Finally, the experimental average distance was compared to that extracted from a molecular modeling investigation.

Materials and Methods

Synthesis and Characterization of Peptides. Melting points were determined using a Leitz (Wetzlar, Germany) model Laborlux 12 apparatus and are not corrected. Optical rotations were measured using a Perkin-Elmer (Norwalk, CT) model 241 polarimeter equipped with a Haake (Karlsruhe, Germany) model D thermostat. Thin-layer chromatography was performed on Merck (Darmstadt, Germany) Kieselgel $60F_{254}$ precoated plates using the following solvent systems: 1, $CHCl_3$−EtOH, 9:1 (EtOH = ethanol); 2, Bu^{n}OH−AcOH−H_2O, 3:1:1 (Bu^{n}OH = *n*-butanol, AcOH = acetic acid); 3, toluene−EtOH, 7:1; 4, EtOAc−PE, 1:3 (EtOAc = ethyl acetate, PE = petroleum ether). The chromatograms were examined by using ultraviolet (UV) fluorescence or developed by chlorine−starch−potassium iodide or ninhydrin chromatic reaction as appropriate. All compounds were obtained in a chromatographically homogeneous state. Mass spectra were recorded for all TOAC-containing peptides by means of a time-of-flight Reflex mass spectrometer using the MALDI ionization tecnique. IR absorption spectra were obtained in KBr pellets on a Perkin-Elmer model 580-B spectrophotometer equipped with a Perkin-Elmer model 3600 IR data station and a model 660 printer.

The free amino acid TOAC and its fluorenyl-9-methyloxycarbonyl (Fmoc) N^{α}-protected derivative were prepared according to published procedures.[2l,8a] Since the acidic and reducing conditions required to remove the *tert*-butyloxycarbonyl (Boc) and benzyloxycarbonyl (Z) groups, respectively, are not compatible with the full integrity of the nitroxide moiety,[8b] the Fmoc N^{α}-protecting group was chosen for the stepwise elongation of the TOAC-containing peptides. The Fmoc group was removed by treatment with a 25% diethylamine solution in CH_2Cl_2. After evaporation of the solvent, the N-terminal free peptide was dissolved in $CHCl_3$ and isolated by elution through a 3-cm bed of silica gel using a $CHCl_3$−EtOH 9:1 mixture.

The Aib and Ala residues were incorporated using the symmetrical anhydride approach (method I), while the TOAC residues were introduced by either the 1-hydroxy-7-aza-benzotriazole (HOAt)-mediated carbodiimide method[9a] (method II) or the acyl fluoride method[9b] (method III). Fmoc-TOAC-F was prepared from the N^{α}-protected amino acid, cyanuric fluoride, and pyridine in CH_2Cl_2 as described in ref 5. The substituted linear template Ac-TOAC-Aib_2-TOAC-Aib-O*t*Bu (**1**) was synthesized from its N-terminal free analogue by treatment with acetic anhydride in CH_2Cl_2.

For the synthesis of the side-chain-substituted cyclic templates **2** and **3,** the linear N^{α}-deprotected pentapeptides were coupled to the cyclo-(Glu-Glu)[4] template by activating the γ-carboxylic groups of the Glu side chains of the DKP with HOAt/carbodiimide (method IV).

The physical properties of the amino acid derivatives and peptides are listed in Table 1. The substituted linear template **1** and cyclic templates **2** and **3** were additionally characterized by amino acid analysis (C. Erba model 3A30 amino acid analyzer, Rodano, Milan, Italy). It is worth noting that TOAC is unstable under the acidic conditions required for the hydrolysis of the −CONH−, −OCONH−, and −COO− bonds, but, after hydrolysis, an area proportional to the quantity of TOAC can still be measured [**1**, Aib, 2.8, Xxx (TOAC), 2.2; **2**, Glu, 2.0, Aib, 7.9, Xxx (TOAC), 2.1; **3**, Glu, 1.9, Ala, 3.8, Aib, 4.2, Xxx (TOAC), 2.2].

Typical coupling procedures used were the following:

Method I. Fmoc-Aib_2-TOAC-Aib_2-O*t*Bu. To a stirred solution of H-Aib-TOAC-Aib_2-O*t*Bu (0.51 g, 1.12 mmol) in 5 mL of anhydrous CH_2Cl_2 was added the symmetrical anhydride of Fmoc-Aib-OH[11] (0.98 g, 1.55 mmol), followed, after 30 min, by 0.085 mL (0.78 mmol) of 4-methylmorpholine (NMM). After the reaction mixture was stirred for 3 days, the solvent was removed under reduced pressure, the residue was dissolved in EtOAc, and the organic layer was washed with 10% $KHSO_4$, water, 5% $NaHCO_3$, and water, dried over Na_2SO_4, filtered, and concentrated under reduced pressure. The peptide was purified by flash chromatography on a silica gel column and eluted with a 96:4 $CHCl_3$/EtOH mixture. Crystallization from EtOAc/PE afforded the product in a 61% yield.

(3) Toniolo, C.; Crisma, M.; Formaggio, F. *Biopolymers (Pept. Sci.)* **1998**, *47*, 153−158.

(4) (a) Bonomo, R. P.; Conte, E.; Impellizzeri, G.; Pappalardo, G.; Purrello, R.; Rizzarelli, E. *J. Chem. Soc., Dalton Trans.* **1996**, 3093−3099. (b) Impellizzeri, G.; Pappalardo, G.; Rizzarelli, E.; Tringali, C. *J. Chem. Soc., Perkin Trans. 2* **1996**, 1435−1440. (c) Bergeron, J. R.; Phanstiel, O., IV; Yao, G. W.; Milstein, S.; Weimar, W. R. *J. Am. Chem. Soc.* **1994**, *116*, 8479−8484. (d) Fusaoka, Y.; Ozeki, E.; Kimura, S.; Imanishi, Y. *Int. J. Pept. Protein Res.* **1989**, *34*, 104−110.

(5) Toniolo, C.; Benedetti, E. *Trends Biochem. Sci.* **1991**, *16*, 350−353.

(6) (a) Karle, I. L.; Balaram, P. *Biochemistry* **1990**, *29*, 6747−6756. (b) Toniolo, C.; Benedetti, E. *Macromolecules* **1991**, *24*, 4004−4009.

(7) (a) Bolin, K. A.; Hanson, P.; Wright, S. J.; Millhauser, G. L. *J. Magn. Reson.* **1998**, *131*, 248−253. (b) Yu, L.; Meadows, R. P.; Wagner, R.; Fesik, S. W. *J. Magn. Reson.* **1994**, *B 104*, 77−80. (c) Kopple, K. D.; Zhu, P. P. *J. Am. Chem. Soc.* **1983**, *105*, 7742−7746. (d) Lord, S. T.; Breslow, E. *Biochemistry* **1980**, *19*, 5593−5602.

(8) (a) Marchetto, R.; Schreier, S.; Nakaie, C. R. *J. Am. Chem. Soc.* **1993**, *115*, 11042−11043. (b) Rozantsev, E. G. In *Free Nitroxyl Radicals*; Ulrich H., Ed.; Plenum Press: New York, 1970; pp 93−115.

(9) (a) Carpino, L. A. *J. Am. Chem. Soc.* **1993**, *115*, 4397−4398. (b) Carpino, L. A.; Sadat Aalaee, D.; Chao, H. G.; DeSelms, R. H. *J. Am. Chem. Soc.* **1990**, *112*, 9651−9652.

(10) (a) Jones, D. S.; Kenner, G. W.; Preston, J.; Sheppard, R. C. *J. Chem. Soc.* **1967**, 6227−6239. (b) Crisma, M.; Valle, G.; Bianco, A.; Formaggio, F.; Toniolo, C. *Z. Kristallogr.* **1996**, *211*, 561−562.

(11) (a) Meienhofer, J.; Waki, M.; Heimer, E. P.; Lambros, T. J.; Makofske, R.; Chang, C. *Int. J. Pept. Protein Res.* **1979**, *13*, 35−42. (b) Valle, G.; Bonora, G. M.; Toniolo, C. *Can. J. Chem.* **1984**, *62*, 2661−2666.

Table 1. Physical Properties of the Amino Acid Derivatives and Peptides

compound	melting point (°C)	recryst. solvent[c]	$[\alpha]^{20}_D$ (deg)[b]	TLC				mass		IR[c]
				R_{F1}	R_{F2}	R_{F3}	R_{F4}	$(M+H)^+$	$(M+Na)^+$	
Fmoc-TOAC-F	oil						0.25			3320, 1838, 1718, 1607, 1522
$(Fmoc\text{-}Aib)_2O$	150−151	EtOAc/PE		0.95		0.65				3395, 1810, 1714, 1513
Z-Aib-O*t*Bu[d]	63−64	Et_2O/PE		0.95	0.95					3372, 1711, 1584, 1563
Fmoc-TOAC-Aib-O*t*Bu	170−171	EtOAc/Et_2O		0.95	0.95	0.50			602	3398, 3313, 1718, 1657, 1521
Z-Aib_2-O*t*Bu[d]	136−137	EtOAc/PE		0.95	0.95					3336, 1693, 1530
Z-Ala-Aib-O*t*Bu[e]	99−100	Et_2O/PE	−29.8	0.75	0.95	0.40				3308, 1736, 1713, 1689, 1676, 1550, 1535
Fmoc-Aib-TOAC-Aib-O*t*Bu	80−82	EtOAc/PE		0.85	0.95	0.45		666	688	3357, 1732, 1702, 1552
Fmoc-TOAC-Aib_2-O*t*Bu	164−165	EtOAc/PE		0.75	0.95	0.35		612	650	3442, 3372, 3333, 1731, 1707, 1689, 1521
Fmoc-TOAC-Ala-Aib-O*t*Bu	98−100	EtOAc/PE	−4.9	0.70	0.95	0.35		653	675	3338, 1728, 1709, 1526
Fmoc-Aib_2-TOAC-Aib-O*t*Bu	188−190	EtOAc		0.70	0.95	0.35		749	772	3359, 1732, 1697, 1671, 1525
Fmoc-Aib-TOAC-Aib_2-O*t*Bu	206−208	EtOAc/PE		0.75	0.95	0.35		695	717	3356, 3330, 1734, 1704, 1683, 1661, 1526
Fmoc-Ala-TOAC-Ala-Aib-O*t*Bu	113−115	EtOAc/PE	−27.9	0.60	0.95	0.35		723	746	3342, 1720, 1672, 1526
Fmoc-TOAC-Aib_2-TOAC-Aib-O*t*Bu	214−215	EtOAc/CH_2Cl_2/PE		0.75	0.95	0.30		949	971	3342, 1729, 1698, 1662, 1525
Fmoc-Aib_2-TOAC-Aib_2-O*t*Bu	226−228	EtOAc/PE		0.60	0.95	0.30		776		3422, 3335, 1684, 1670, 1527
Fmoc-Aib-Ala-TOAC-Ala-Aib-O*t*Bu	128−129	EtOAc/PE	−2.8	0.60	0.95	0.30		809	830	3339, 1731, 1667, 1526
Ac-TOAC-Aib_2-TOAC-Aib-O*t*Bu (**1**)	273−275	CH_2Cl_2/PE		0.30	0.85	0.05		768	790	3436, 3317, 1730, 1662
cyclo-[Glu(Aib_2-TOAC-Aib_2-O*t*Bu)]$_2$ (**2**)	176−178	EtOAc/PE	+14.5	0.10	0.80	0.05		1448	1470	3324, 1716, 1664, 1528
cyclo-[Glu(Aib-Ala-TOAC-Ala-Aib-O*t*Bu)]$_2$ (**3**)	159−161	MeOH/H_2O	+29.5[f]	0.25	0.80	0.00		1393	1415	3323, 1729, 1657, 1537

[a] EtOAc = ethyl acetate, PE = petroleum ether, Et_2O = diethyl ether, MeOH = methanol. [b] $c = 0.5$, methanol. [c] The solid-state IR absorption spectra were obtained in KBr pellets (only bands in the 3450−3300 and 1850−1500 cm^{-1} regions are reported). [d] Reference 10a. [e] Reference 10b. [f] $c = 0.25$, methanol.

Method II. Fmoc-TOAC-Aib_2-TOAC-Aib-O*t*Bu. To a suspension of Fmoc-TOAC-OH[2l,8a] (0.18 g, 0.41 mmol) and HOAt (0.058 g, 0.42 mmol) in 3 mL of anhydrous CH_2Cl_2 at 0 °C was added 1-(3-(dimethylamino)propyl)-3-ethylcarbodiimide hydrochloride (EDC·HCl) (0.1 g, 0.52 mmol). When the suspension became clear, H-Aib_2-TOAC-Aib-O*t*Bu (0.18 g, 0.35 mmol), dissolved in 3 mL of anhydrous CH_2Cl_2, was added, followed, after 30 min, by 0.046 mL (0.41 mmol) of NMM. The reaction mixture was allowed to stir for 3 days at room temperature. The solvent was removed under reduced pressure, the residue was dissolved in EtOAc, and the organic layer was washed with 10% $KHSO_4$, water, 5% $NaHCO_3$, and water, dried over Na_2SO_4, filtered, and concentrated under reduced pressure. The peptide was purified by flash chromatography on a silica gel column and eluted with a 95:5 $CHCl_3$/EtOH mixture. Crystallization from EtOAc/CH_2Cl_2/PE afforded the product in a 49% yield.

Method III. Fmoc-TOAC-Aib-O*t*Bu. To a stirred solution of Fmoc-TOAC-F (2.42 g, 5.53 mmol) in 10 mL of anhydrous CH_2Cl_2 at 0 °C was added H-Aib-O*t*Bu (1.46 g, 9.2 mmol) [obtained from Pd-catalyzed hydrogenation in methanol (MeOH) of the corresponding Z-protected amino acid ester[10a] (2.70 g, 9.2 mmol)], dissolved in 3 mL of anhydrous CH_2Cl_2, and the solution was allowed to stir overnight at room temperature. The solvent was removed under reduced pressure, the residue was dissolved in EtOAc, and the organic layer was washed with 10% $KHSO_4$, water, 5% $NaHCO_3$, and water, dried over Na_2SO_4, filtered, and concentrated under reduced pressure. Crystallization from EtOAc/PE afforded the product in a 65% yield.

Method IV. Cyclo-[Glu(Aib_2-TOAC-Aib_2-O*t*Bu)]$_2$ (2). To a solution of cyclo-(Glu-Glu)[4] (0.021 g, 0.08 mmol) and HOAt (0.028 g, 0.21 mmol) in 2 mL of DMF at 0 °C was added EDC·HCl (0.044 g, 0.23 mmol). Then, H-Aib_2-TOAC-Aib_2-O*t*Bu (0.11 g, 0.19 mmol), dissolved in 2 mL of DMF, was added, followed, after 30 min, by 0.018 mL (0.16 mmol) of NMM. After the solution was stirred at room temperature overnight, the solvent was removed in vacuo, the residue was dissolved in EtOAc, and the organic layer was washed with 10% $KHSO_4$, water, 5% $NaHCO_3$, and water, dried over Na_2SO_4, filtered, and concentrated under reduced pressure. The peptide was purified by flash chromatography on a silica gel column and eluted with a 95:5 $CHCl_3$/EtOH mixture. Crystallization from EtOAc/PE afforded the product in a 61% yield.

FTIR Absorption. FTIR absorption spectra were recorded with a Perkin-Elmer model 1720 X spectrophotometer, nitrogen flushed and equipped with a sample-shuttle device, at 2 cm^{-1} nominal resolution, averaging 100 scans. Solvent (baseline) spectra were obtained under the same conditions. Cells with path lengths of 0.1, 1.0, and 10 mm (with CaF_2 windows) were used. Spectrograde deuteriochloroform (99.8% D) was purchased from Fluka.

X-ray Diffraction. Pale yellow crystals of the linear pentapeptide **1** were grown from a MeOH/Et_2O solution by slow evaporation. A single crystal of approximate dimensions 0.4 × 0.4 × 0.1 mm was mounted on the tip of a glass capillary. Cell parameters were determined from 48 well-centered reflections in the 11−22° θ range. Data collection was performed by using a Philips PW1100 four-circle diffractometer and graphite-monochromated Cu Kα radiation ($\lambda = 1.541\ 84$ Å), $\theta-2\theta$ scan mode up to $2\theta = 100°$, h from −10 to 10, k from −18 to 20, l from 0 to 24. The crystal did not significantly diffract above $2\theta = 100°$ (1.0 Å resolution).

The structure was solved by direct methods (SHELXS 86 program).[12a] The asymmetric unit turned out to be made of two independent peptide molecules (**A** and **B**) and four cocrystallized water molecules. Refinement was carried out on F^2, using the full data set and the SHELXL 97[12b] program. In both independent molecules, the C-terminal −O*t*Bu group is disordered, and it was refined on two sets of positions, with population parameters of 0.60 and 0.40 for the major and minor conformers, respectively, in molecule **A**, and 0.66 and 0.34, respectively, in molecule **B**. For molecule **B** only, the disorder could be traced to include also the C═O group of Aib(15). The refinement was carried out by full-matrix block least-squares, with all non-hydrogen atoms anisotropic, and allowing the positional parameters and the anisotropic

(12) (a) Sheldrick, G. M. *SHELXLS 86. Program for the Solution of Crystal Structures*; University of Göttingen: Göttingen, Germany, 1986. (b) Sheldrick, G. M. *SHELXL 97. Program for the Refinement of Crystal Structures*; University of Göttingen: Göttingen, Germany, 1997. (c) Nardelli, M. *J. Appl. Crystallogr.* **1995**, *28*, 659. (d) Spek, A. L. *Acta Crystallogr.* **1990**, *A46*, C-34, MS-02.01.05.

Table 2. Crystal Data for Pentapeptide **1** Dihydrate

empirical formula	$C_{38}H_{67}N_7O_9 \cdot 2H_2O$
mol wt	802.0
temp (K)	293(2)
crystal system	triclinic
space group	$P\bar{1}$
a (Å)	10.435(2)
b (Å)	20.878(3)
c (Å)	24.207(3)
α (deg)	68.4(1)
β (deg)	89.1(1)
γ (deg)	82.8(1)
V (Å^3)	4862.1(13)
Z	4
molecules/asymmetric unit	2
density (g/cm^3) (calcd)	1.096
abs coeff (mm^{-1})	0.660
F(000)	1744
no. of collected reflcns	9347
no. of independent reflcns	9311
no. of reflcns with $I \geq 2\sigma(I)$	3950
R_1 [on $F \geq 4\sigma(F)$]	0.0834
wR_2 [on F^2, all data]	0.2472
R_{int}	0.0264
no. of data/restraints/parameters	9311/268/1070
goodness of fit	0.896
max shifts/esd's	0.712
max/min $\Delta\rho$ (e/Å^3)	+0.424/−0.307

displacement parameters of the non-hydrogen atoms to refine at alternate cycles. Restraints were applied to the 1−2 and 1−3 interatomic distances involving atoms of the disordered groups, as well as to their anisotropic displacement parameters. Hydrogen atoms of the peptide molecules were calculated at idealized positions, and during the refinement they were allowed to ride on their parent atom, with U_{iso} set equal to 1.2 (or 1.5 for methyl groups) times the U_{eq} of their carrying atom. The positions of the hydrogen atoms bound to the water molecules were recovered from a ΔF map, and they were not refined. Other relevant crystallographic data are listed in Table 2. Geometrical calculations were performed with the PARST[12c] and PLATON[12d] programs.

Electron Spin Resonance. Continuous wave spectra of the peptides were recorded using a Bruker ESR-380 X-band spectrometer equipped with a TE_{102} cavity and a ER4111 variable-temperature unit. The temperatures at which this unit regulates were checked against a Cernox ceramic thermocouple purchased from and calibrated by Lakeshore Cryonics. Allowed transitions at 300 and at 118 K were recorded with a center field of 3357 G, typically with a sweep width of 150 G, a modulation frequency of 100 kHz, a modulation amplitude of 1 G, a time constant of 82 ms, a conversion time of 164 ms, and a receiver gain of 1.00×10^4, at 2.7 mW, with four scans acquired for each spectrum. Half-field spectra were recorded at 118 K at a center field of 1677 G, typically with a sweep width of 200 G, a modulation frequency of 100 kHz, a modulation amplitude of 5 G, a time constant of 328 ms, a conversion time of 328 ms, and a receiver gain of 2.00×10^4, at 84 mW, with up to 12 scans acquired for each spectrum. Integrated intensities for both spectral regions were determined via double integration of the recorded derivative-mode spectra. For the half-field signals, a third-order polynomial baseline correction was determined using 35 G of baseline at both edges of the absorption mode spectrum and subtracting this polynomial from the entire spectrum prior to the second integration. Integrated intensities of the half-field transitions were normalized by dividing by the number of scans acquired, the solution concentration, and the square-root of the spectrometer power. Relative intensity values for use in calculations according to the procedure reported by Eaton and co-workers[13] were obtained from allowed transitions recorded at 118 K and from half-field transitions at the same temperature. The ratio of the doubly integrated intensities was taken after normalizing for receiver gain, number of scans, and square root of the microwave power. Samples were prepared in a glassing solvent mixture consisting of 9:1 (v/v) MeOH/EtOH. Samples for room-temperature measurements (40 μL) were sealed into glass capillaries (100 μL). Samples for half-field measurements were prepared using 300 μL of this mixed solvent solution placed in 4-mm-i.d. quartz sample tubes and quickly frozen in liquid nitrogen to form a glass. The samples were directly and immediately placed in the cooler spectrometer cavity for spectral acquisition. Spectrograde MeOH and EtOH were obtained from Fischer, 2,2,2-trifluoroethanol (TFE) from Aldrich, and 1,1,1,3,3,3-hexafluoro-2-propanol (HFIP) from Sigma.

(13) Eaton, S. S.; More, K. M.; Sawant B. M.; Eaton, G. R. *J. Am. Chem. Soc.* **1983**, *105*, 6560−6567.

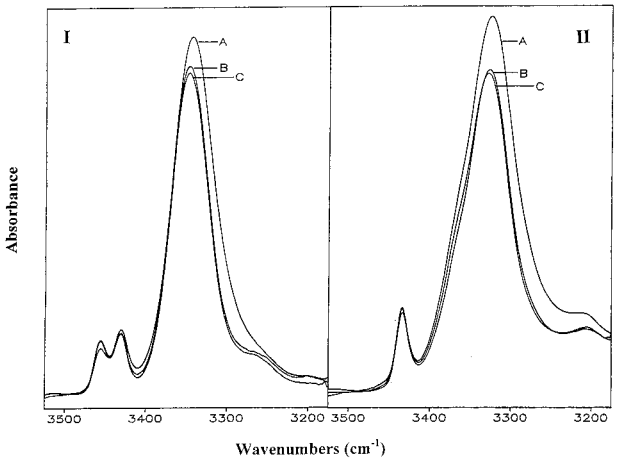

Figure 2. Normalized FTIR absorption spectra (N−H stretching region) of Ac-TOAC-Aib$_2$-TOAC-Aib-O*t*Bu (**1**) (I) and cyclo-[Glu-(Aib$_2$-TOAC-Aib$_2$-O*t*Bu)]$_2$ **2** (II) in 10 (A), 1 (B), 0.1 mM (C) $CDCl_3$ solution, respectively.

Molecular Modeling. Computer models were built using MOLMOL[14] and a library modified to incorporate the TOAC and Aib residues. Calculations required to appropriately transform the coordinates for inclusion and inspection of the models were aided by use of MOLMOL on a Silicon Graphics workstation.

Results and Discussion

FTIR Absorption. The conformational preferences of the substituted linear and cyclic templates **1**−**3** were investigated in $CDCl_3$ using FTIR absorption. The most significant results are illustrated in Figure 2 and listed in Table 3.

The three spectra are characterized by weak bands in the 3457−3430 cm^{-1} region (free N−H groups) and more intense bands (shoulders) at 3370−3324 cm^{-1} (H-bonded N−H groups).[15a,b] In particular, the more complex absorption of **2** and **3** can be rationalized as arising from an overlapping of the amide N−H stretching modes of cyclo-(Glu-Glu) at 3380 cm^{-1} and the pentapeptides anchored to the cyclic skeleton at 3350 cm^{-1} (data not shown). At any event, in all of the compounds, even at the highest dilution examined, the intensity of the 3347−3324 cm^{-1} band is remarkable, thereby suggesting the occurrence of a large population of highly intramolecularly H-bonded species.[15a] This finding indicates that pentapeptide **1** and the peptide segments covalently bound to the DKP rings are arranged in a well-ordered conformation. Furthemore, for all peptides the analysis of the C═O stretching region reveals a strong band at 1664 ± 2 cm^{-1}, typical of H-bonded amide carbonyls in a 3_{10}-helica1 conformation, in addition to weaker bands (shoulders) at 1729−1728 and 1679 ± 3 cm^{-1}, assigned

(14) Koradi, R.; Billeter, M.; Wütrich, K. *J. Mol. Graphics* **1996**, *14*, 51−55.

(15) (a) Mizushima, S.; Shimanouchi, T.; Tsuboi, M.; Souda, R. *J. Am. Chem. Soc.* **1952**, *74*, 270−271. (b) Palumbo, M.; Da Rin, S.; Bonora, G. M.; Toniolo, C. *Makromol. Chem.* **1976**, *177*, 1477−1492. (c) Kennedy, D. F.; Crisma, M.; Toniolo, C.; Chapman, D. *Biochemistry* **1991**, *30*, 6541−6548.

Table 3. Infrared Absorption Data for Peptides **1**−**3** in $CDCl_3$[a]

compound	N−H stretching region[b]	C═O stretching region[b]
Ac-TOAC-Aib$_2$-TOAC-Aib-O*t*Bu (**1**)	*3457*, *3430*, **3347**	*1729*, 1682, **1662**
cyclo-[Glu(Aib$_2$-TOAC-Aib$_2$-O*t*Bu)]$_2$ (**2**)	*3435*, 3370,[c] **3329**	*1728*, 1676,[c] **1666**
cyclo-[Glu(Aib-Ala-TOAC-Ala-Aib-O*t*Bu)]$_2$ (**3**)	*3434*, 3364,[c] **3324**	*1728*, 1677,[c] **1662**

[a] Concentration, 1.0 mM. [b] Values shown in italic type represent weak bands; values shown in boldface type represent strong bands. [c] Shoulder.

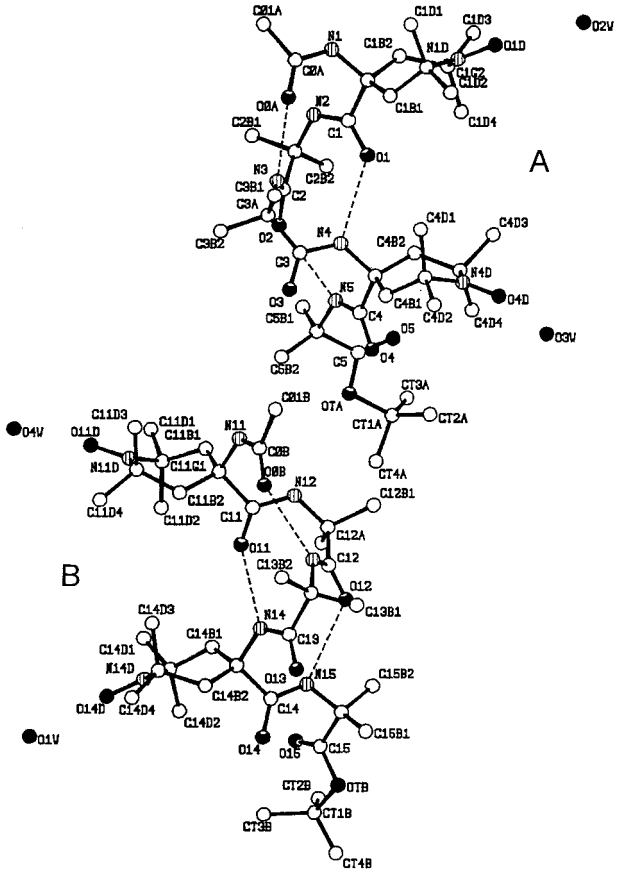

Figure 3. X-ray diffraction structure of the two independent molecules (**A** and **B**) in the asymmetric unit of Ac-TOAC-Aib$_2$-TOAC-Aib-O*t*Bu (**1**) with atom numbering. The intramolecular H-bonds are indicated by dashed lines.

to the *tert*-butyl ester carbonyl and free amide carbonyls, respectively.[15c]

In summary, the present FTIR absorption investigation has provided convincing evidence that the linear pentapeptide **1**, and the peptide segments anchored to the side chains of the cyclo-(Glu-Glu) template adopt a helical conformation in a solvent of low polarity.

X-ray Diffraction. The molecular and crystal structures of the terminally blocked pentapeptide Ac-TOAC-Aib$_2$-TOAC-Aib-O*t*Bu (**1**) were determined in the crystal state by X-ray diffraction. A view perpendicular to the helix axis of the two independent molecules (**A** and **B**) in the asymmmetric unit is illustrated in Figure 3. Amino acid residues are numbered from 1 to 5 in molecule **A** and from 11 to 15 in molecule **B**. For clarity, for each molecule, only the major conformer of the disordered C-terminal −O*t*Bu group is shown. Relevant backbone torsion angles[16] are given in Table 4. In Table 5, the intra- and intermolecular H-bond parameters are listed. Owing to the space group symmetry, in the crystal each molecule has a centrosymmetric counterpart of opposite handedness.

Table 4. Relevant Backbone Torsion Angles (deg) for Molecules **A** and **B** of Pentapeptide **1**

angle	molecule **A**	molecule**B**
ω_0	177.3(7)	−175.3(7)
ϕ_1	55.7(9)	−54.2(9)
ψ_1	29.1(8)	−31.9(8)
ω_1	178.9(6)	−177.6(6)
ϕ_2	55.4(8)	−57.3(8)
ψ_2	22.5(8)	−23.1(8)
ω_2	−177.4(5)	−179.9(5)
ϕ_3	47.8(7)	−51.9(8)
ψ_3	32.5(8)	−28.8(8)
ω_3	176.2(6)	−178.6(6)
ϕ_4	57.1(8)	−53.4(8)
ψ_4	35.8(8)	−38.7(9)
ω_4	−177.8(6)	179.0(7)
ϕ_5	−58.7(10)	47.2(13),[a] 74.0(14)[b]
ψ_5	133.0(19),[a] 146.0(13)[b]	−145.0(15),[a] −121(2)[b]
ω_5	177.0(12),[a] 175.8(19)[b]	−171.1(14),[a] 168(2)[b]

[a] Major conformer. [b] Minor conformer.

Bond lengths and bond angles (deposited) are in general agreement with those reported for the peptide unit,[17] the O*t*Bu ester,[18] and the Aib[19] and TOAC[2i,l,20] residues.

Molecule **A** and molecule **B** are left-handed and right-handed 3_{10}-helices, respectively, both stabilized by three consecutive and strong[21] intramolecular H-bonds between the C═O group of residue i and the N−H group of residue $i + 3$, typical of β-turns.[22] For both molecules, the first intramolecular H-bond, starting from the N-terminus, involves the carbonyl oxygen atom of the acetyl moiety and the peptide nitrogen atom of Aib(3) (O0A···N3 for molecule **A**, O0B··N13 for molecule **B**). The absolute values of the ϕ,φ backbone torsion angles, as averaged for the four helical residues of both molecules **A** and **B**, are 54.1°,30.3°, close to those typical for a peptide 3_{10}-helix (57°, 30°).[5] In both molecules **A** and **B**, the C-terminal −O*t*Bu group is disordered over two conformations. In molecule **B**, the disorder also includes the C═O group of the C-terminal Aib residue. In all of the four rotamers, the C-terminal Aib residue adopts a semi-extended conformation (regions F/F* of the conformational space),[23] with the sign of the ϕ torsion angle opposite to that of the preceding residues. In the two molecules,

(16) IUPAC−IUB Commission on Biochemical Nomenclature. *Biochemistry* **1970**, *9*, 3471−3479.

(17) (a) Benedetti, E. In *Chemistry and Biochemistry of Amino Acids, Peptides and Proteins*; Weinstein, B., Ed.; Dekker: New York, 1982; pp 105−184. (b) Ashida, T.; Tsunogae, Y.; Tanaka, I.; Yamane, T. *Acta Crystallogr.* **1987**, *B43*, 212−218.

(18) Schweizer, W. B.; Dunitz, J. D. *Helv. Chim. Acta* **1982**, *65*, 1547−1554.

(19) (a) Paterson, Y.; Rumsey, S. M.; Benedetti, E.; Némethy, G.; Scheraga, H. A. *J. Am. Chem. Soc.* **1981**, *103*, 2947−2955. (b) Valle, G.; Crisma, M.; Formaggio, F.; Toniolo, C.; Jung, G. *Liebigs Ann. Chem.* **1987**, 1055−1060.

(20) Flippen-Anderson, J. L.; George, C.; Valle, G., Valente, E.; Bianco, A.; Formaggio, F.; Crisma, M.; Toniolo, C. *J. Pept. Protein Res.* **1996**, *47*, 231−238.

(21) (a) Ramakrishnan, C.; Prasad, N. *Int. J. Protein Res.* **1971**, *3*, 209−231. (b) Taylor, R.; Kennard, O.; Versichel, W. *Acta Crystallogr.* **1984**, *B40*, 280−288. (c) Görbitz, C. H. *Acta Crystallogr.* **1989**, *B45*, 390−395.

(22) (a) Venkatachalam, C. M. *Biopolymers* **1968**, *6*, 1425−1436. (b) Toniolo, C. *CRC Crit. Rev. Biochem.* **1980**, *9*, 1−44. (c) Rose, G. D.; Gierasch, L.; Smith, J. P. *Adv. Protein Chem.* **1985**, *37*, 1−109.

(23) Zimmerman, S. S.; Pottle, M. S.; Némethy, G.; Scheraga, H. A. *Macromolecules* **1977**, *10*, 1−9.

Table 5. Intra- and Intermolecular H-Bond Parameters for Pentapeptide **1** (Molecules **A** and **B**)

	donor D−H	acceptor A	symmetry operations of A	distance (Å) D···A	distance (Å) H···A	angle (deg) D−H···A
			Intramolecular			
molecule **A**	N3−H	O0A	*x*, *y*, *z*	2.972(7)	2.13	164.4
	N4−H	O1	*x*, *y*, *z*	3.022(7)	2.17	171.2
	N5−H	O2	*x*, *y*, *z*	2.922(8)	2.18	143.7
molecule **B**	N13−H	O0B	*x*, *y*, *z*	2.959(8)	2.13	161.7
	N14−H	O11	*x*, *y*, *z*	3.004(7)	2.15	169.2
	N15−H	O12	*x*, *y*, *z*	2.961(8)	2.21	146.2
			Intermolecular			
peptide−water	N1−H	O1W	*x*, *y*, *z*	2.981(7)	2.14	164.6
	N2−H	O2W	*x*, *y*, *z*	2.988(8)	2.16	162.6
	N11−H	O3W	*x*, *y*, *z*	2.938(7)	2.09	168.0
	N12−H	O4W	*x*, *y*, *z*	2.979(8)	2.15	161.4
water−peptide	O1W−H1A	O13	*x*, *y*, *z* − 1	2.782(7)	1.96	173.3
	O1W−H1B	O14D	*x* + 1, *y*, *z* − 1	2.922(7)	2.29	133.6
	O2W−H2A	O14	*x*, *y*, *z* − 1	2.800(8)	2.00	159.0
	O2W−H2B	O1D	*x* −1, *y*, *z*	2.831(8)	2.03	163.2
	O3W−H3A	O3	*x*, *y*, *z*	2.777(7)	2.06	144.2
	O3W−H3B	O4D	*x* −1, *y*, *z*	2.880(7)	2.07	162.9
	O4W−H4A	O4	*x*, *y*, *z*	2.806(8)	1.98	167.8
	O4W−H4B	O11D	*x* + 1, *y*, *z*	2.856(9)	2.36	119.1

a significant deviation of the amide, peptide, and ester ω torsion angles ($|\Delta\omega| > 5°$) from the ideal trans planar conformation (180°) is observed only for the ester ω_5 torsion angles of both conformers of molecule **B**. For three out of the four C-terminal conformers, the *tert*-butyl ester disposition with respect to the preceding $C^{\alpha}-N$ bond is intermediate between the *synperiplanar* and *synclinal* conformations, while it is *synperiplanar* for the minor conformer of molecule **B**.[24] For each independent molecule **A** and **B**, the main difference between the major and the minor conformers is found in the disposition of the C-terminal *tert*-butyl group with respect to the preceding C′−O bond. This disposition is fully staggered in the major conformer, while in the minor conformer one of the $C-CH_3$ bonds is eclipsed (*synperiplanar*).

In each molecule, the piperidinyl rings of the two TOAC residues, separated by one complete turn of the 3_{10}-helix, are oriented roughly perpendicular to the helix axis and nearly parallel to each other, the angle between normals to the average ring plane being 12.8(2)° and 13.8(2)° in molecules **A** and **B**, respectively. The angle between the two N−O• groups is 39.3(4)° in molecule **A** and 43.5(5)° in molecule **B**. The distance between midpoints of the two N−O• bonds is 7.376(7) and 7.388(7) Å in molecules **A** and **B**, respectively. The latter values are about 0.06 Å larger than the corresponding distance found in the X-ray diffraction structure of the 3_{10}-helical peptide *p*BrBz-TOAC-(L-Ala)$_2$-TOAC-L-Ala-NH*t*Bu (*p*BrBz = *p*-bromobenzoyl; NH*t*Bu = *tert*-butylamino).[2l,20] In each peptide molecule of the present structure, the two N−O• bonds diverge more than in the structure mentioned above,[2l,20] owing to their involvement in H-bonds with the cocrystallized water molecules. It is reasonable to assume that such an effect induced on the N−O• groups by the water molecules may be relaxed in solution.

Interestingly, in the left-handed helical molecule **A**, the piperidinyl ring of TOAC(1) is found in a conformation close to the $^2T_6$ twist-boat disposition, while the ring conformation of TOAC(4) is intermediate between the $B_{3,6}$ boat and the $^2T_6$ twist-boat dispositions. Conversely, the ring conformations observed in the right-handed helical molecule **B** are intermediate between the $^{3,6}B$ boat and the $^6T_2$ twist-boat dispositions for TOAC(11) while intermediate between the $B_{2,5}$ boat and the $^6T_2$ twist-boat dispositions for TOAC(14). It should be noted that, in this classification, we considered the ring atom sequence $C^{\alpha}-C^{\beta 1}-C^{\gamma 1}-N^{\delta}-C^{\gamma 2}-C^{\beta 2}$, where $C^{\beta 1}$ refers to the *pro-S* C^{β} atom. The ring-puckering parameters are the following: Q_T = 0.648(7) Å, ϕ_2 = 261.9(5)°, θ_2 = 89.4(6)° for TOAC(1) and Q_T = 0.619(6) Å, ϕ_2 = 287.6(5)°, θ_2 = 97.6(5)° for TOAC(4) of molecule **A**; Q_T = 0.622(7) Å, ϕ_2 = 102.3(6)°, θ_2 = 88.2(6)° for TOAC(11) and Q_T = 0.635(6) Å, ϕ_2 = 74.6(6)°, θ_2 = 96.5(6)° for TOAC(14) of molecule **B**.[25]

The endocyclic torsion angles about the $C^{\beta}-C^{\gamma}$ bonds exhibit values in the range ±40−±57°, close to those of cyclohexane (±54°−±55°)[26a] and piperidine (±48°−±52°).[26b] All of the other endocyclic torsion angles are found in the range ±1°−±46° (in each ring, the lowest value is observed for one of the torsion angles about the $C^{\gamma}-N^{\delta}$ bonds). Such an observation is common to other six-membered nitroxide derivatives[2i,l,20] and indicates that the piperidine rings are most flattened in the N^{δ} part.

The angles between the normal to the average ring plane and the $C^{\alpha}-N$ and $C^{\alpha}-C'$ bonds are in the range 30°−43°, indicating that both the α-amino and the α-carbonyl ring substituents occupy a bisectional position,[27] as usually observed for TOAC residues in linear derivatives and peptides.[2i,l,20]

In the packing mode of the Ac-TOAC-Aib$_2$-TOAC-Aib-O*t*Bu (**1**) molecules, there are no direct peptide−peptide intermolecular H-bonds. Rather, a complex network of H-bonds is observed involving the four cocrystallized water molecules.[28] In addition, in both peptide molecules **A** and **B**, the NH groups of TOAC(1)/TOAC(11) and Aib(2)/Aib(12), the carbonyl groups of Aib(3)/Aib(13) and TOAC(4)/TOAC(14), and the nitroxide oxygen atoms of TOAC(1)/TOAC(11) and TOAC(4)/TOAC(14) act as intermolecular H-bonding donors or acceptors.

(24) Dunitz, J. H.; Strickler, P. In *Structural Chemistry and Molecular Biology*; Rich, A., Davidson, N., Eds.; Freeman: San Francisco, 1968; pp 595−602.

(25) Cremer, D.; Pople, J. A. *J. Am. Chem. Soc.* **1975**, *97*, 1354−1358.

(26) (a) Bixon, M.; Lifson, S. *Tetrahedron* **1967**, *23*, 769−784. (b) Cygler, M.; Markovicz, T.; Skolimowski, J.; Skowronski, R. *J. Mol. Struct.* **1980**, *68*, 161−171.

(27) Luger, P.; Bülow, R. *J. Appl. Crystallogr.* **1983**, *16*, 431−432.

(28) (a) Yang, C. Y.; Brown, J. N.; Kopple, K. D. *Int. J. Pept. Protein Res.* **1979**, *14*, 12−20. (b) Jeffrey, G. A.; Maluszynska, H. *Acta Crystallogr.* **1990**, *B46*, 546−549. (c) Görbitz, C. H.; Etter, M. *Int. J. Pept. Protein Res.* **1992**, *39*, 93−110.

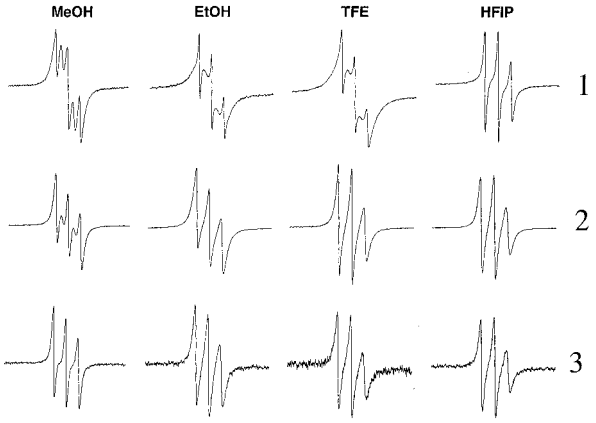

Figure 4. ESR spectra (150 G scan width) of Ac-TOAC-Aib$_2$-TOAC-Aib-O*t*Bu (**1**), cyclo-[Glu(Aib$_2$-TOAC-Aib$_2$-O*t*Bu)]$_2$ (**2**), and cyclo-[Glu(Aib-Ala-TOAC-Ala-Aib-O*t*Bu)]$_2$ (**3**) in four alcohols at 300 K.

Electron Spin Resonance. The solvent-dependent unfolding of **1**−**3** was investigated at room temperature using ESR spectroscopy. Spectra taken in each of four solvents are shown from left to right in Figure 4 in order of each solvent's demonstrated ability to support helical structures in short peptides (MeOH > EtOH > TFE > HFIP).[2k] Specifically, alcohols with greater polarity and H-bonding capability as donors (e.g., HFIP) are known to destabilize helical structures in these compounds. The doubly labeled pentapeptide, **1**, shows the largest solvent-dependent spectroscopic change, exhibiting a strong, five-line *J*-coupling pattern in MeOH which reveals the close inter-nitroxide spatial proximity expected for a highly helical conformation. This coupling gradually decreases through the solvent series until, in HFIP, no evidence of the five-line pattern can be seen. Similar *J*-coupling, although weaker, is observed for **2** in MeOH that is quickly lost in the other solvents, while **3** shows little evidence of such coupling. More tellingly, though, is a comparison among the three compounds in the most destructuring solvent (HFIP). In this solvent, the ESR spectra lines for **2** and **3** are both broader than those of **1**. This uniform broadening of all three nitroxide hyperfine lines indicates that the total contribution of inter-nitroxide coupling (either dipolar or exchange coupling) is stronger for **2** and **3** than for **1** (we note that longer correlation times, as might be expected for **2** and **3** if more motionally restricted, would preferentially broaden only the high-field hyperfine line). This increased spectral broadening is consistent with a shorter inter-nitroxide distance for both **2** and **3** than for **1**.

Considering a limiting case constrained only by covalent connectivity, a completely extended backbone conformation for **1** would put the inter-nitroxide spacing *r* at approximately 11−12 Å. This represents an extreme upper bound for the average inter-nitroxide distance in **2** and **3** in HFIP. Local steric interactions restrict how closely **1** can approach such an extended conformation, so the distance is probably significantly less than this upper bound in all three compounds.

A more quantitative measure of the average inter-nitroxide distance results from measurements of the half-field signal intensity.[13,29] The integrated intensity of this signal is proportional to r^{-6}, and it can arise from intramolecular as well as intermolecular dipolar coupling. Extrapolation of signal intensities to infinite dilution reveals only the intramolecular coupling, with the intermolecular contribution manifest as a negative slope for the extrapolation. Figure 5 shows this extrapolation for **2**

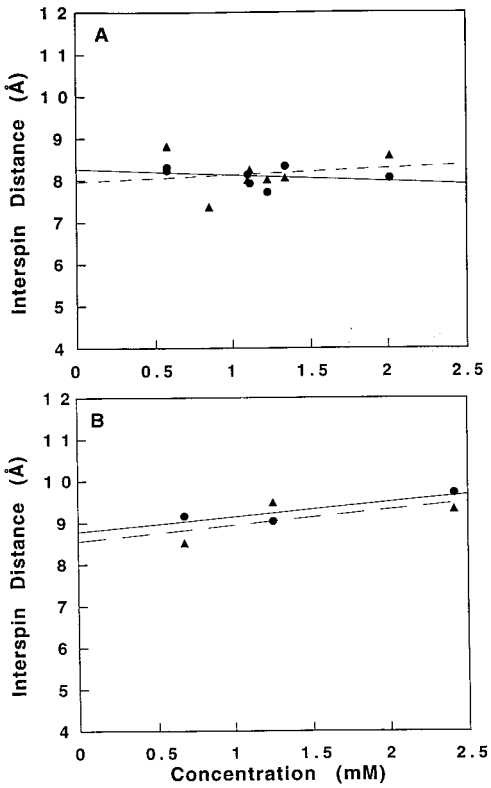

Figure 5. Plots of the interspin distance vs peptide concentration for cyclo-[Glu(Aib$_2$-TOAC-Aib$_2$-O*t*Bu)]$_2$ (**2**) (A) and cyclo-[Glu(Aib-Ala-TOAC-Ala-Aib-O*t*Bu)]$_2$ (**3**) (B), determined by half-field measurements. In both parts A and B, ▲ and (---) correspond to the interspin distance (relative intensity), and ● and (—) to the interspin distance (normalized intensity). The lines through the data points correspond to linear regression (least-squares) fits.

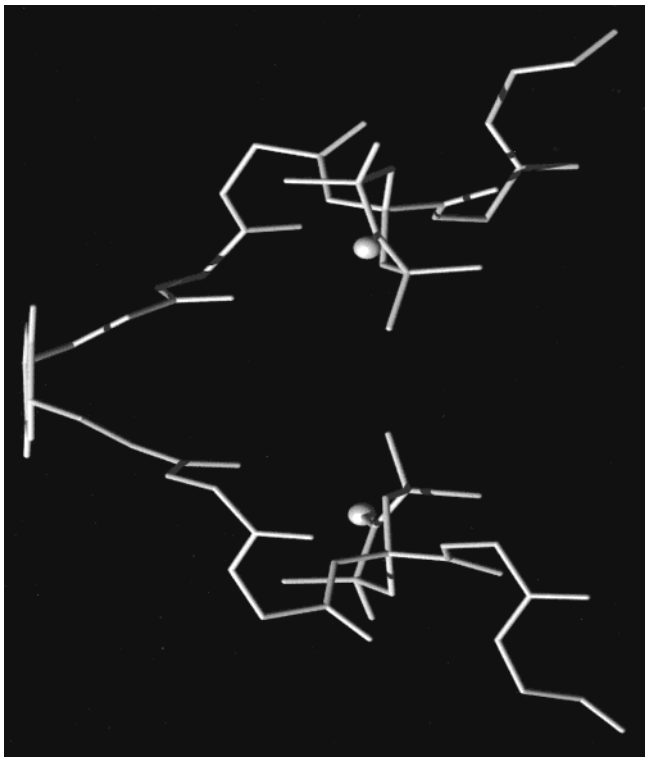

Figure 6. Molecular model of cyclo-[Glu(Aib$_2$-TOAC-Aib$_2$-O*t*Bu)]$_2$ (**2**), with Aib methyl groups omitted for clarity.

(29) Anderson, D. J.; Hanson, P.; McNulty, J.; Millhauser, G.; Monaco, V.; Formaggio, F.; Crisma, M.; Toniolo, C. *J. Am. Chem. Soc.* **1999**, *121*, 6919−6927.

and **3** in a helix-supporting 9:1 MeOH/EtOH solvent glass at 120 K, and similar results for a series of 3_{10}-helical peptides analogous to **1** have recently been published.[29] Two independent calibrations for the intensity-to-distance conversion have been employed: an instrument-independent calibration using a formula developed by Eaton and co-workers,[13] and another using measurements performed on doubly labeled TOAC-containing peptides of known structure studied in our laboratory. The lack of significant negative slope in any of the extrapolated lines in Figure 5 suggests little intermolecular contribution to the half-field signal for these samples over the concentration range investigated. Distances determined from both calibrations agree within experimental error. The average for **2** is 8.1 Å, while for **3** it is slightly longer (8.7 Å). The half-field results, taken together with evidence of both significant *J*-coupling in **2** and persistent biradical broadening for both **2** and **3**, indicate that these chains do approach one another.

Molecular Modeling. Figure 6 illustrates how this approach might be arranged. The model was constructed with each helix held in 3_{10}-helical conformation ($\phi = -57°$, $\psi = -30°$)[5] and with the cyclo-(Glu-Glu) side-chain torsion angles ($\chi_1 = 30°$, $\chi_2 = 180°$, $\chi_3 = -150°$) arranged such that the inter-nitroxide distance (average of the N···N and O···O distances) is comparable to that indicated by half-field measurements (8.4 Å). No significant steric helix−helix contacts exist in this model, allowing for the possibility that molecules with helix−helix contact and shorter inter-nitroxide distances represent a significant population contributing to the ensemble average.

Conclusions

In this paper, we reported the design, chemical synthesis, and conformational analysis of two simple two-helix model systems fully based on peptide building blocks. The conformationally restricted template is the cyclo-homopeptide cyclo-(Glu-Glu) containing two side-chain carboxyl functionalities, to which two copies of the same 3_{10}-helical pentapeptide tails are tethered through amide covalent bonds. Each pentapeptide is characterized by one stable free-radical-containing TOAC residue. By exploiting these two molecular bundles, *for the first time* we detected by ESR in a *fully synthetic* construct an inter-helix interaction between spins located far away in the amino acid sequence. This phenomenon is reduced by an increase of the solvent polarity that is responsible for a destabilization of the peptide helical structures. The experimentally determined interspin distance matches well that obtained from a molecular modeling investigation.

The results presented in this study strongly support our contention that the semi-rigid, helicogenic TOAC residue is a valuable tool for the detection of interactions between an appropriately tailored, TOAC-based, synthetic peptide inhibitor or hormone analogue and its side-chain spin-labeled, site-directed Cys mutant enzyme or receptor counterpart.

Acknowledgment. D.J.A. and G.L.M. were supported by a grant from the National Institutes of Health (GM 46870).

Supporting Information Available: Tables of crystal data and structure refinement, atomic coordinates, isotropic and anisotropic displacement parameters, bond lengths and angles, hydrogen coordinates, torsion angles, relevant backbone and side-chain torsion angles, and intra- and intermolecular parameters for **1** (PDF). X-ray crystallographic data, in CIF format, are also available. This material is available free of charge via the Internet at http://pubs.acs.org.

JA992079H